arXiv:1704.03127v1 [stat.ME] 11 Apr 2017

Feature Sensitive Curve Registration by Maximizing Kernel based Matching Scores

DIBYENDU BHAUMIK[1] and RADHENDUSHKA SRIVASTAVA[2] and DEBASIS SENGUPTA[3]

[1]*Corresponding Author; Assistant Adviser, Department of Statistics and Information Management, Reserve Bank of India, C9, 6th Floor, Bandra Kurla Complex, Bandra (East), Mumbai 400051, Maharashtra, IndiaE-mail:* dbhaumik@rbi.org.in

[2]*Assistant Professor, Department of Mathematics, Indian Institute of Technology, Powai, Bombay 400076, Maharashtra, IndiaE-mail:* rsrivastava22@gmail.com

[3]*Professor, Applied Statistics Unit, Indian Statistical Institute, 203, Barrackpore Trunk Road, Kolkata 700108, West Bengal, IndiaE-mail:* sdebasis@isical.ac.in

Given two sets of functional data having a common underlying mean function but different degrees of distortion in time measurements, we provide a method of estimating the time transformation necessary to align (or 'register') them. This method, which we refer to as kernel-matched registration, is based on maximizing a kernel-based measure of alignment. We prove that the proposed method is consistent under fairly general conditions. Simulation results show superiority of the performance of the proposed method over two existing methods. The proposed method is illustrated through the analysis of three paleoclimatic data sets.

Keywords: Alignment function, Consistency, Curve alignment, Functional data, Ice core data, Measure of alignment, Warping function.

1. Introduction

Consider functional data arising from observations recorded at a sequence of time points. The task of aligning multiple but similar sets of functional data by possibly nonlinear adjustment to their time scales is often referred to as 'registration'. The problem of registration is also important in image and video processing, where multiple dimensions are involved. In the one dimensional case, the need for registration has been felt in broadly two types of problems. For longitudinal growth data, often viewed as a common pattern expressed differently through different individuals with their diverse scales of evolution, the need for registration arises from the quest for the common pattern. In this type of problems, the number of individuals is generally much more than the number of observations per individual. On the other hand, for paleoclimatic data on historic movement of climate variables, the need for registration arises from the notion that the recorded 'time' contains estimation error that might come in the way of collation of information from multiple sets of data. In these applications, the number of observations per data set is much more than the number of data sets to be time-aligned or registered. There may even be only two data sets

for alignment. In this paper, we address the second type of problems, and focus on registration of one data set with respect to another. Registration may be used in this type of problems either as a necessary step towards improved inference of a common underlying function, or merely for the sake of comparison. In this paper, we regard curve registration as an end in itself.

As a motivating example, consider the atmospheric concentration of carbon dioxide for the past 400,000 years constructed from two ice cores extracted from two different locations in Antarctica namely lake Vostok and EPICA dome [15, 13], plotted in Fig. 3 (top-left panel). The peaks in the EPICA dome data (many of which are sharp) precede those in the lake Vostok data during the initial and later parts of the time span, while the reverse happens in the middle part. It suggests the possible existence of a non-linear relationship between the time values of the two data sets.

It is possible to use the sharp peaks and valleys in the data series, often identified as 'landmarks', for the purpose of registration. A simplistic method would be to identify specific landmarks of one data set that correspond to the landmarks of the other data set, and use a piecewise linear time transformation that permits the alignment of the two sets of landmarks. Kneip and Gasser [8] proposed a method of registration under the constraint that the identified landmarks should match. The identification of matching landmarks is generally done manually. This is a disadvantage of landmark-assisted registration. Bigot [1] proposed an automated landmark-based method which estimates time transformation function by using the pairs of matched times of landmarks as input, which are separately obtained in an automated manner. The performance of this multiple-step method may be limited by the non-use of information other than landmarks and possible accumulation of estimation errors at each step.

One may also hold the view that paying too much attention to the details may cause distortion, as observation times in either of the data sets may miss the actual peaks of the underlying continuous time phenomenon. In that case, the method of registration should not utilize these features as such. Instead, there should be emphasis on strengthening of inference through the pooling of local information. Smoothing is a common technique for such pooling. There are several methods that make use of smoothing: continuous monotone registration [16], dynamic time warping [20, 21], registration by local regression [10], maximum likelihood registration through parametric modeling of the time transformation [17, 5], self-modelling warping [4], shape invariant model based registration [2], functional convex synchronization model based registration [11], pair-wise curve synchronization [19], and functional principal component based registration [18, 9].

However, sharp peaks and valleys in the data may be characteristics of the underlying common function, as appears to be the case for the paleoclimatic example. In that case it may be unwise to ignore the information contained in them. Ramsay and Li [16] suggested that a landmark based preliminary registration may be further refined through their method. The other methods mentioned above may also be used for refinement. Manual identification of some matching landmarks in the two data sets (after preliminary smoothing) have been used as input to the methods proposed by Kneip and Gasser [8] and Kneip and Engel [7]. All said and done, smoothing based methods may be unable to take full advantage of the information contained in sharp changes in the data, as smoothing blurs these features. There may be a better way of pooling local information, specifically for the purpose of registration.

James [6] proposed a new method based on matching of 'functional moments', intended to

capture landmarks or local features. This method, as well as the functional principal components used by Silverman [18] and Kneip and Ramsay [9], rely on pooling of information from many replicates, for estimation of the population characteristics. These methods may be appropriate for longitudinal growth data, where sufficient replicates are available, but not for applications where only a pair of data sets need to be registered.

In this paper, we propose a new method of registering one functional data set with respect to another, where the requirement of pooling local information is built into the task of alignment. The method neither relies on local smoothing nor uses manually identified landmarks.

We model the observations of the two data sets as,

$$y_1(t) = m(t) + \epsilon_1(t); \quad y_2(t) = m(g(t)) + \epsilon_2(t),$$

where m is the underlying mean function, g is the requisite time transformation, and ϵ_1 and ϵ_2 are random error terms. The task of registration is essentially that of estimating g that aligns the two sets of data. Note that the above model would not be suitable for data sets representing observations on different variables (e.g., paleoclimatic data sets on temperature and carbon dioxide). On the other hand, any generalization of the above model for applicability to different variables would involve additional estimation, which is redundant when the observed variables are in fact identical. Thus, such a generalization can only be achieved at the cost of inefficient utilization of the available information.

In § 2, we propose a new estimator of the time transformation function g, by maximizing a 'measure of alignment' of two functional data sets. The maximization is done over an appropriate class of transformations. This measure of alignment is designed to capture the information contained in the entire set of data, including locations of sharp variation. We show that it possesses some desired characteristics. The method is automated as it does not require manual identification of landmarks. Identifiability of g with respect to the chosen model, under appropriate conditions, is proved in § 3.

Many of the existing methods of estimation of the time transformation have been proposed without establishing their consistency. Rønn [17] and Gervini and Gasser [5] have proved the consistency of their methods when the number of subjects goes to infinity. Following Kneip and Engel [7], Wang and Gasser [21], and Gervini and Gasser [4], we have established the consistency of our estimator as the numbers of observations in the two data sets go to infinity. This result, reported in § 3, holds when the time transformation is chosen from a class of functions satisfying some general conditions.

Results of a simulation study, to demonstrate the performance of the estimator chosen from a particular class, are reported in § 4. The method is illustrated in § 5 through the analysis of several real data sets. Some concluding remarks are provided in § 6.

2. Model and Methodology

Let $\{(t_1, Y_{t_1}), \ldots, (t_{n_1}, Y_{t_{n_1}})\}$ and $\{(s_1, Y'_{s_1}), \ldots, (s_{n_2}, Y'_{s_{n_2}})\}$ be two sets of functional data, arising from the model

$$\begin{aligned} Y_{t_i} &= m(t_i) + \epsilon_1(t_i) \quad (i = 1, \ldots, n_1) \\ Y'_{s_j} &= m(g_0(s_j)) + \epsilon_2(s_j), \quad (j = 1, \ldots, n_2) \end{aligned} \tag{2.1}$$

where m is an underlying location function that is continuous, and g_0 is an unknown time transformation function, which is continuous and strictly increasing. The terms ϵ_1 and ϵ_2 represent additive random measurement errors, which have mean zero.

Now, let us define, for any given continuous and strictly increasing transformation function g, the functional

$$L_n(g) = \frac{\frac{1}{n_1 n_2}\sum_{i=1}^{n_1}\sum_{j=1}^{n_2}\frac{1}{h_1}K_1\left(\frac{t_i - g(s_j)}{h_1}\right)\frac{1}{h_2}K_2\left(\frac{Y_{t_i} - Y'_{s_j}}{h_2}\right)}{\frac{1}{n_1 n_2}\sum_{i=1}^{n_1}\sum_{j=1}^{n_2}\frac{1}{h_1}K_1\left(\frac{t_i - g(s_j)}{h_1}\right)}, \tag{2.2}$$

where $n = n_1 + n_2$, K_1 and K_2 are kernel functions that are probability densities, and h_1 and h_2 are the corresponding bandwidths. The above functional can be interpreted as a weighted sum of the terms $(1/h_2)K_2\{(Y_{t_i} - Y'_{s_j})/h_2\}$ $(i = 1, \ldots, n_1;\ j = 1, \ldots, n_2)$, which can be seen as matching scores between Y_{t_i}'s and Y'_{s_j}'s. The weights depend on g. Note that when $g = g_0$, for every pair of i and j such that $g(s_j)$ is close to t_i, the continuity of m ensures that $Y_{t_i} - Y'_{s_j}$ is expected to be small. Therefore, for $g = g_0$, large values of $(1/h_2)K_2\{(Y_{t_i} - Y'_{s_j})/h_2\}$ are expected to occur together with large values of their weights. This may not be the case when $g \neq g_0$. In § 3, we show that under some general conditions, the probability limit of $L_n(g)$ attains its maximum value if and only if $g = g_0$.

Thus, $L_n(g)$ may be interpreted as a measure of alignment or a kernel-matched overall score.

Let us now examine the roles of the bandwidth parameters h_1 and h_2 in the above measure. A small value of h_1 makes the weight for a given i and j nearly equal to zero, unless t_i is very close to $g(s_j)$. Thus, only a few weights can be substantial. When h_1 is large, weights can be substantial for more combinations of i and j. Thus, h_1 controls the effective number of weights in the weighted sum in (2.2). On the other hand, h_2 controls the penalty for discrepancies between Y_{t_i} and Y'_{s_j}. A very large value of h_2 might make $L_n(g)$ insensitive to changes in g, as there would not be enough penalty for mismatch between Y_{t_i} and Y'_{s_j}. A very small value of h_2 would make $L_n(g)$ unstable, as $(1/h_2)K_2\{(Y_{t_i} - Y'_{s_j})/h_2\}$ would be nearly zero for most of the combinations of i and j.

We define the proposed estimator of the function g_0 as

$$\hat{g}_n = \arg\max_{g \in \mathbb{G}} L_n(g), \tag{2.3}$$

where $L_n(g)$ is as defined in (2.2) and $\mathbb{G}$ is a suitable class of continuous and strictly increasing functions that includes the true transformation function g_0.

As for choices of the bandwidths, one can select h_1 as a fraction of the average horizontal separation between successive observations in the lesser dense data set and h_2 as a fraction of the combined range of the observed variable. Some guidelines are given in § 4.

The objective function $L_n(g)$ automatically rewards candidate transformation functions that map peaks of one data set into the corresponding peaks of the other. On the other hand, if a peak is missing from one of the data sets, then it does not penalize the 'correct' transformation any more than a similar alternative candidate (i.e., a marginally different transformation). Therefore, the estimator $\hat{g}_n$ should be able to utilize these 'landmarks' automatically for registration.

3. Consistency

Let the errors $\epsilon_1(t_i)$ and $\epsilon_2(s_j)$ and the time points t_i and s_j $(i = 1, \ldots, n_1;\ j = 1, \ldots, n_2)$ be mutually independent sets of samples from the probability density functions f_{ϵ_1}, f_{ϵ_2}, f_1, and f_2 having supports over $(-\infty, \infty)$, $(-\infty, \infty)$, $[a, b]$ (for $0 \leq a < b$), and $[c, d]$ (for $0 \leq c < d$) respectively.

We assume that m in model (2.1) is a continuous function defined over $[0, \infty)$. We also presume that it is not flat or it does not fluctuate too much. In order to ensure this, we formally stipulate that for every $y \in \left[\min_{t\in[p,q]} m(t), \max_{t\in[p,q]} m(t)\right]$, the set $\{t :\ m(t) = y,\ t \in [p, q]\}$ has a finite number of elements where $[p, q]$ is any given interval.

We now make a stronger assumption about g_0 in model (2.1). We assume that g_0 is differentiable almost everywhere with derivative bounded from below by a positive number, which implies that g_0 is strictly increasing and continuous. Estimation of g_0 makes sense only if $g_0([c, d])$ has a substantial overlap with $[a, b]$. We, therefore, assume that $g_0([c, d]) \cap [a, b]$ includes a non-empty open interval. We also need to ensure that there is no ambiguity about g_0 in model (2.1). Let $\mathbb{G}_0$ be the class of all functions g defined over $[c, d]$, differentiable almost everywhere with derivative bounded from below by a positive number, such that the set $S_g = g^{-1}([a, b]) \cap [c, d]$ contains a non-empty open interval and that g agrees with g_0 at least at one point in $S_{g_0} \cap S_g$. By construction, $g_0 \in \mathbb{G}_0$. Our first result establishes the identifiability of g_0 (within $\mathbb{G}_0$) with respect to model (2.1).

Theorem 3.1. *Let m, g_0, and $\mathbb{G}_0$ be as described above. If $g \in \mathbb{G}_0$ is such that $m(g(s)) = m(g_0(s))$ for all $s \in S_g \cap S_{g_0}$, then $S_g = S_{g_0}$ and $g(s) = g_0(s)$ for all $s \in S_{g_0}$.*

The consistency of $\hat{g}_n$ needs to be established as the sample size in both the data sets go to infinity [7, 21, 4]. As a first step, we establish the point-wise convergence of the functionals L_n on $\mathbb{G}_0$ after making the following assumptions.

***Assumption* 3.1.** The densities f_{ϵ_1}, f_{ϵ_2}, f_1, and f_2 are continuous and bounded; f_{ϵ_1} and f_{ϵ_2} are symmetric about zero and are strictly unimodal at zero; f_1 and f_2 are positive over the interior of their supports.

***Assumption* 3.2.** The kernels K_1 and K_2 are continuous and bounded probability density functions defined over the real line.

This condition is satisfied by all the popular kernels viz. uniform, triangular, Epanechnikov, biweight, Gaussian, and so on.

***Assumption* 3.3.** The sample sizes n_1 and n_2 are such that $n_1/n \to \xi$ for some $\xi \in (0, 1)$, as $n \to \infty$.

***Assumption* 3.4.** The bandwidths are such that $h_i \to 0$ and $n_i h_i \to \infty$ as $n \to \infty$ $(i = 1, 2)$.

Theorem 3.2. *Let m, g_0, and $\mathbb{G}_0$ be as described at the beginning of this section. Then, under Assumptions 3.1–3.4, for any function $g \in \mathbb{G}_0$, $L_n(g)$ tends to $L(g)$ in probability as $n \to \infty$, where*

$$L(g) = \frac{\int_{-\infty}^{\infty}\int_{0}^{\infty} f_1(g(y))f_2(y)f_{\epsilon_1}(v - m(g(y)) + m(g_0(y)))f_{\epsilon_2}(v)dydv}{\int_{0}^{\infty} f_1(g(y))f_2(y)dy}. \tag{3.1}$$

We now show that this limiting functional is maximized only by the correct transformation function.

Theorem 3.3. *Suppose m, g_0, and $\mathbb{G}_0$ are as described at the beginning of this section. Then, under Assumption 3.1,*

(a) $L(g) \leq L(g_0)$ for all $g \in \mathbb{G}_0$,
(b) If $L(g) = L(g_0)$ for some $g \in \mathbb{G}_0$, then $g = g_0$ over S_{g_0}.

The next step is to establish the uniform convergence of L_n, for which we need a stronger condition on $\mathbb{G}_0$ that enforces compactness. Let us define a metric on $\mathbb{G}_0$ viz., $d(g_1, g_2) = \sup_{x\in[c,d]} |g_1(x) - g_2(x)| = \|g_1 - g_2\|$.

***Assumption* 3.5.** The class $\mathbb{G}$ in (2.3) is a compact subset of $\mathbb{G}_0$ in the metric space $(\mathbb{G}_0, d)$ and it includes g_0.

An example of $\mathbb{G}$ that satisfies Assumption 3.5 is the subset of functions g of $\mathbb{G}_0$ with bounded slope.

***Assumption* 3.6.** The kernels K_1 and K_2 are bounded away from zero on a given closed interval and have bounded first order derivatives.

The Gaussian kernel satisfies this condition.

Theorem 3.4. *Let m, g_0, and $\mathbb{G}_0$ be as described at the beginning of this section. Then under the Assumptions 3.1–3.6, $\sup_{g\in\mathbb{G}} |L_n(g) - L(g)|$ tends to zero in probability as $n \to \infty$.*

We now establish that the sequence of maximum values of the functionals L_n converges to the value of L at its maximizer, g_0.

Theorem 3.5. *Let m, g_0, and $\mathbb{G}_0$ be as described at the beginning of this section. Then under the Assumptions 3.1–3.6, $L_n(\hat{g}_n)$ tends to $L(g_0)$ in probability as $n \to \infty$.*

Finally we establish the consistency of our estimator.

Theorem 3.6. *Let m, g_0, and $\mathbb{G}_0$ be as described at the beginning of this section. Then under the Assumptions 3.1–3.6, $\hat{g}_n$ tends to g_0 in probability as $n \to \infty$.*

4. Simulation of performance

4.1. Methods compared

Even though we have proposed a general class of estimators in § 2 and established their consistency in § 3, we need to focus on a specific member of that class in order to simulate the performance. We chose $\mathbb{G}$ as the vector space generated by linear B-spline basis functions with equidistant knot points over $[a, b]$. In order to ensure that all the weights in (2.2), which are the ratios of kernels involving g, are defined for every trial g in the iterative maximization process, we chose non-vanishing Gaussian kernel for K_1. The other kernel K_2 was also chosen as Gaussian, though any kernel would have served the purpose. We chose h_1 as 50 per cent of the average horizontal separation between successive observations in the lesser dense data set and h_2 as 10 per cent of the range of combined Y-values of both the data sets. These choices worked well in the simulations. The method of steepest ascent was used to maximize (2.2). In order to provide an initial iterate to the maximization algorithm, we programmatically mapped significant peaks and valleys of the two data sets.

We carried out simulations to compare the performance of the above implementation of the proposed kernel-matched registration method with two other methods.

1. The first method for comparison was continuous monotone registration. The `fda` package of `R` was used for computations, which involved two steps. In the first step, smooth curves were computed from noisy data sets by using the routine `smooth.basis`, while the warping function was estimated in the second step by using `register.fd`. Both the computations used a common B-spline basis system which was specified by the routine `create.bspline.basis` with default choice of order of b-spline basis functions (4) and number of equidistant break-points same as the number of knot-points used for the proposed method. Functions were estimated by penalizing curvatures with a common choice of the smoothing parameter (λ) as 10^{-4}, as suggested in [16].
2. The second method was self-modelling registration [4]. MATLAB codes provided by the authors were used for computations with default choices for the number of random starts (20) and the order of splines (3). The sets of data chosen for simulations revealed the existence of approximately seven prominent features. Therefore, following suggestions by the authors, the plausible value of number of components, q, was chosen to vary from 7 to 12, which also satisfied the prescribed rule of thumb (i.e. $q <$ square root of number of observations). The suggested possible values of the number of basis functions, p, were $3q$ or $4q$. The final choice was made by the cross-validation algorithm proposed by the authors.

These methods were selected for comparison mostly on account of applicability to the data at hand and availability of codes. The wavelet based automated method of [1] requires size of the input data sets to be equal to powers of 2, which made it unsuitable for the data we considered.

4.2. Simulation Design

The choice of data for simulation was motivated by the paleoclimatic data set that exhibited sharp changes. We chose lake Vostok data on atmospheric concentration of carbon dioxide (with 283 data points, range of time-values $I = [2.342, 414.085]$ and standard deviation of Y-values $s = 28.7$) described in § 1, as the base data set for our simulation exercises. The function m was obtained by linearly interpolating between these data points. Time-values of simulation data sets were selected keeping adequate margins from the boundaries of I so that transformed time-values did not exceed the boundaries. We conducted Monte Carlo simulations in four different scenarios under model (2.1) (with $n_1 = n_2 = 250$) as described below:

Scenario 1. We randomly selected a sub-set D of 250 data points from the base set. In every simulation run, we constructed the pair of data sets as follows:

(a) Time values of both the data sets were kept same as those in D;

(b) The time transformation g_0 in (2.1), applied on the time values of the second data set, was chosen as linear spline with six equidistant knots over the range of time-values of D i.e. at 11.013, 84.737, 158.461, 232.185, 305.909, and 379.633, plotted in Fig. 1 namely,

$$\begin{aligned} g_0(t) \quad = \quad & 0.950t + 0.115(t - 11.013)_+ - 0.230(t - 84.737)_+ \\ & +0.430(t-158.461)_+ - 0.630(t-232.185)_+ \\ & +0.830(t-305.909)_+ - 1.617(t-379.633)_+ \quad t \in I \end{aligned} \tag{4.1}$$

where u_+ is u for positive u and zero otherwise and I is as defined at the beginning of this subsection;

(c) Additive errors were generated afresh from the normal distribution with mean $\mu = 0$ and standard deviation $\sigma = 0.05s$ where s is as defined earlier in this subsection, for both the data sets separately;

Scenario 2. The 250 time points as well as the additive errors for each data set were generated afresh for each simulation run. In this case, the distributions f_1 and f_2 described in § 3 were uniform over some $J \subset I$, while the distributions f_{ϵ_1}, f_{ϵ_2} were normal with $\mu = 0$, $\sigma = 0.05s$. The function g_0 was as in scenario 1.

Scenario 3. This set-up was the same as in Scenario 1, except that g_0 was chosen as the identity function plus a periodic function, plotted in Fig. 1 viz.,

$$g_0(t) = t + 0.05t \sin\left(\frac{3\pi t}{c}\right) \quad t \in I \tag{4.2}$$

where c is the upper boundary of I.

Scenario 4. This set-up was the same as in scenario 2, except that g_0 was as in scenario 3.

Scenario 1 offers an opportunity to assess the performance of the proposed method when $\mathbb{G}$ includes g_0. We chose 21 equidistant knots in our search space of B-splines, so that the g_0 with six equidistant knots becomes a special case. For other scenarios and data analyses, number of

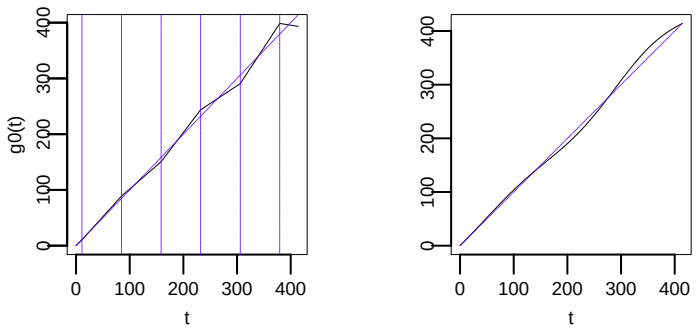

Figure 1. Time transformation functions g_0 (solid lines) in simulations against identity (dashes): linear spline (left) and periodic (right); Vertical dotted lines indicate knot-locations of the linear spline

equidistant knots were chosen as 10 times of the fifth root of the size of the larger data set, as prescribed in Eubank [3], which was found to work well. For continuous monotone registration, we adopted the same formula to decide on number of break-points across all scenarios and in data analyses.

The MATLAB programs for self-modelling registration require values of the functions to be registered at a common set of time points, which is met only in scenario 1 and 3. Therefore, simulation results for this method are reported only for these two scenarios.

The performance of the estimators of g_0 were studied in terms of (a) point-wise bias, (b) point-wise standard deviation, (c) point-wise mean squared error, and (d) average of the integrated mean squared error normalized by the squared norm of the true function, defined for each simulation run as

$$\frac{\frac{1}{S}\sum_{j=1}^{S}\int_I(\hat{g}_j(t)-g_0(t))^2dt}{\int_I g_0^2(t)dt}$$

where S was the number of independent runs of the simulation and $\hat{g}_j$ is the estimate of g_0 at the jth run. We used Simpson's rule to evaluate these definite integrals.

4.3. Results

The results of the simulations based on 1000 independent runs for each of the scenarios, are shown in Fig. 2. Continuous monotone registration produced absurd estimates of g_0 for three particular simulation runs in both of the scenarios 2 and 4. Therefore, results for these scenarios were based on remaining 997 runs for the method. Self-modelling registration, on the other hand, did not converge for one simulation run in scenario 3, which was also similarly treated.

It is observed that, the proposed estimator has, in general, smaller bias, standard deviation, and mean squared error as compared to other methods. In self-modelling registration, warping functions are constrained to be identity at the boundaries of J. This may be sensible for growth data. However, in applications such as the paleoclimatic data considered here, it may not be the

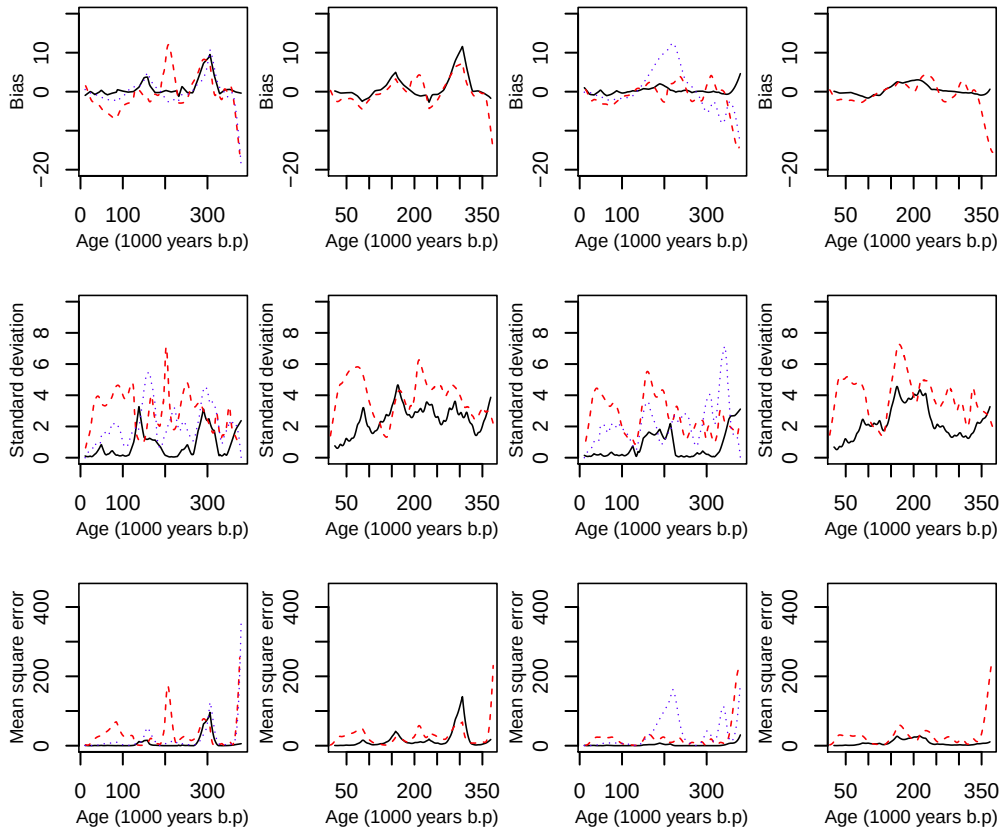

Figure 2. Point-wise bias, standard deviation, and mean squared error of the estimators of g_0 in simulations by continuous monotone registration (dashes), self-modelling registration (dotted lines) and kernel-matched registration (solid lines) under scenario 1 (first column), scenario 2 (second), scenario 3 (third), and scenario 4 (last column)

Table 1. Average normalized integrated mean square error normalized by the squared norm ($\times 10^{-3}$)

Method	Scenario 1	Scen. 2	Scen. 3	Scen. 4
Cont. mon. registration	0.656	0.567	0.422	0.605
Self-modelling registration	0.361	–	0.689	–
Kernel-matched registration	0.154	0.361	0.038	0.164

case. Higher bias of the g_0 estimator towards the right extreme of the timescale was due to this constraint. It is observed in Table 1 that the kernel-matched registration method had uniformly smaller average normalised integrated mean squared errors across all the scenarios.

5. Analysis of ice core data

Here we considered paleoclimatic data on the atmospheric concentration of (i) carbon dioxide, and (ii) methane [15, 12] as determined from air-bubbles trapped in ice cores collected over Lake Vostok and at EPICA Dome in Antarctica, and (iii) average annual temperature deviations [15, 14], which were reconstructed from deuterium contents at various depths of ice cores obtained at these two sites. Table 2 gives an idea of the volume and magnitude of the variables of these data sets.

Table 2. Some descriptive statistics of the data sets

	Data set 1: Vostok		Data set 2: EPICA Dome	
Data	Size	Range(Y-Value)	Size	Range(Y-Value)
Carbon dioxide	283	182.2-298.7	537	183.8-298.6
Methane	457	318-773	1,545	342-907
Temp. deviations	3,310	(-)9.39-3.23	5,028	(-)10.58-5.46

We chose to align the data set from EPICA dome with that from lake Vostok using two registration methods namely, the proposed kernel-matched registration and continuous monotone registration. Parameters of these methods for data analyses were chosen as in the previous section. We could not apply the method of self-modelling registration for the above data sets, since it requires the nominal observation times in the two data sets to coincide.

Alignments of the data sets and the estimates of g_0 for the three pairs of data sets, produced by the two methods, are plotted in Fig. 3.

The average squared distance between the interpolated curves before and after registration by the two methods, computed over a grid of size 1000 over the time range, are reported in Table 3. It is observed that kernel-matched registration method produced shorter distance between the registered curves as compared to continuous monotone registration.

Table 3. Average squared difference between the pairs of data sets

	Carbon dioxide	Methane	Temp. dev.
Pre-alignment	266.09	3,739.06	3.04
Post-alignment:			
Continuous monotone registration	76.22	2,355.14	1.66
Kernel-matched registration	20.48	1,297.87	1.31

6. Discussion

In this paper, we have proposed a new method of registration of one functional data set with another, by optimizing an empirical kernel-based measure of alignment. If there are sharp variations in the data, the proposed method is able to utilize them, without requiring prior identification of

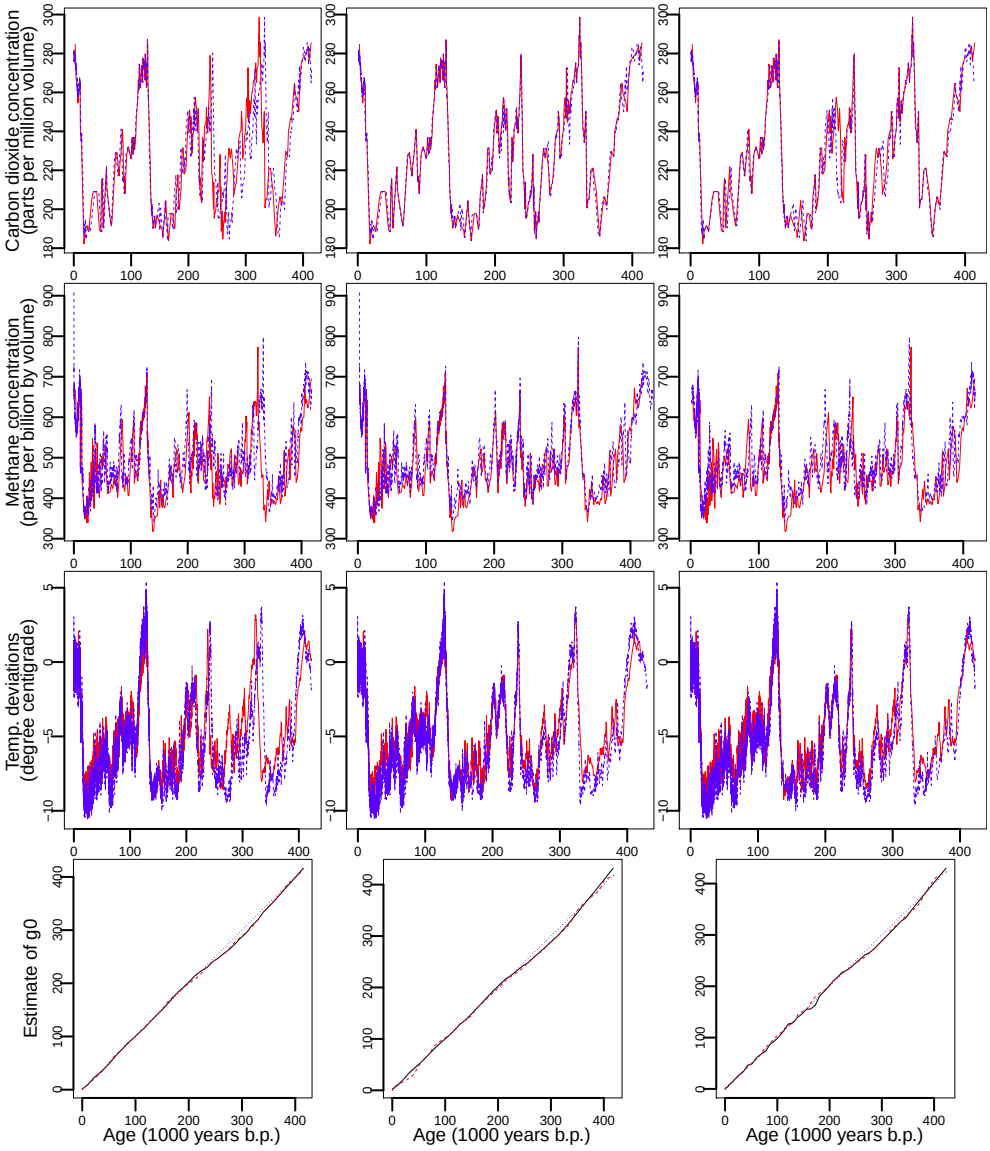
Carbon dioxide concentration (parts per million volume)
Methane concentration (parts per billion by volume)
Temp. deviations (degree centigrade)
Estimate of g0
Age (1000 years b.p.)
Age (1000 years b.p.)
Age (1000 years b.p.)

Figure 3. Atmospheric concentration of carbon dioxide (1st row, left), methane (2nd row, left) and average annual temperature deviations (3rd row, left) constructed from lake Vostok (solid lines) and EPICA dome (dashes) ice cores; Alignment produced by the kernel-matched registration (rows 1-3, middle) and continuous monotone registration (rows 1-3, right); Fourth row: Estimates of g_0 for carbon dioxide (left), methane (middle), and temperature (right) by kernel-matched registration (solid lines) and continuous monotone registration (dashes) against identity (dotted lines)

landmarks. Since the method does not use any pre-smoothing, it does not suffer from any loss of information that might occur due to smoothing. On the other hand, the measure of alignment (2) ensures that the proposed method makes use of the main strength of smoothing, namely pooling of information from neighbouring observations.

The present implementation of the method, in the form of R codes, is available from the authors on request. This implementation permits registration of data sets with possibly unequal, irregularly spaced and large number of samples. This implementation is based on some specific choices, e.g., use of the class of B-splines with uniformly spaced knot points as candidate time transformation functions, and steepest ascent for optimization. However, none of these choices is necessary in the general set-up used for proving the consistency of the proposed class of estimators.

There are indeed some limitations of the proposed approach. When there are many sharp changes in the data, the iterative algorithm may run into spurious local maxima, particularly when the bandwidth parameter h_1 in (2) is small. Such problems may be mitigated by replacing steepest ascent with a probabilistic search algorithm such as simulated annealing. On the other hand, when the data sets do not have sharp changes, the proposed method may not be very sensitive to alterations in the transformation function. The guideline on the choice of bandwidths (particularly h_2) given here may not be applicable for those problems. The proposed method would be completely unsuitable for longitudinal data with many individuals but relatively fewer observations per individual.

The alignment provided by the proposed method is likely to change if the data sets for registration are interchanged. One can choose the solution that produces smaller average of squared difference between the pair of registered data sets. When there are more than two data sets to be registered, the proposed method has to be used multiple times on pairs of data, possibly after identifying one of the data sets as reference for registration. This reference data set may also be selected on a trial basis, and the candidate leading to the best overall alignment may be selected as reference data set at the end. Alternatively, the two-step approach suggested by Tang and Müller [19] may be used.

The proposed method can be used as a tool for structural averaging (which amounts to estimating the function m in model (1)). Large sample properties of the resulting estimator of m and its performance in relation to competing methods need to be studied in future.

Registration of two sets of functional data on different variables (e.g., paleoclimatic data on temperature and carbon dioxide) is sometimes needed for the purpose of studying the relationship between them. The method presented here is not readily applicable to this problem. However, an adaptation may be possible by inserting an unknown amplitude parameter in one of the two equations of model (1). This problem is another possible direction of future work in this area.

Supplementary material

Supplementary material includes the detailed proof of Theorem 3.2.

Appendix A: Proofs

With reference to Assumption 3.1, let the real number M_f be a common upper bound of the densities f_1, f_2, f_{ϵ_1}, and f_{ϵ_2}. With reference to Assumptions 3.2 and 3.6, let the positive real numbers c, M_K, M'_K be such that $0 < c \leq K_i(x) \leq M_K$ and $|K'_i(x)| \leq M'_K$ $(i = 1, 2)$.

Proof of Theorem 3.1. Let $g \in \mathbb{G}_0$ be such that $g(\alpha) = g_0(\alpha)$ for some $\alpha \in S_{g_0} \cap S_g$, $m(g(s)) = m(g_0(s))$ for all $s \in S_{g_0} \cap S_g$, and yet $g(s) \neq g_0(s)$ for some $s \in S_{g_0} \cap S_g$. We can presume, without loss of generality, that $g(s) < g_0(s)$. Let us assume, for now, $\alpha < s$. Then the set $\{t : m(t) = m(g_0(s))\} \cap [g_0(\alpha), g_0(s)]$ has at least two elements, $g(s)$ and $g_0(s)$. Let $t^{(1)} < \cdots < t^{(k)}$ be the ordered elements of this set. Clearly, $g_0(s) = t^{(k)}$. Let $g(s) = t^{(i)}$ for some $i < k$.

In order that the functions $m(g(u)) - m(g(s))$ and $m(g_0(u)) - m(g_0(s))$ coincide for all $u \in [\alpha, s]$, these functions should have exactly the same number of zero crossings over this interval. However, from what we have already observed, the first function has exactly i zero-crossings, while the second function has exactly k zero-crossings, and $i < k$. Therefore, the two functions must differ somewhere on $[\alpha, s]$.

Similarly, if $\alpha > s$, the set, $\{t : m(t) = m(g(s))\} \cap [g(s), g(\alpha)]$ has at least two elements viz., $g(s)$ and $g_0(s)$. If $s^{(1)} < \cdots < s^{(l)}$ be the ordered elements of this set, then $g(s) = s^{(1)}$ and $g_0(s) = s^{(j)}$ for some $j > 1$. By similar arguments, the two functions namely $m(g(u)) - m(g(s))$ and $m(g_0(u)) - m(g_0(s))$, which have been presumed to coincide for all $u \in [s, \alpha]$, must differ somewhere on $[s, \alpha]$ as the first function has exactly l zero-crossings, while the second has exactly $l - j + 1$.

This contradicts the presumption that $g(s) \neq g_0(s)$ for some $s \in S_g \cap S_{g_0}$. Thus, $g = g_0$ over $S_g \cap S_{g_0}$.

The continuity of g and g_0, together with their equality over $S_g \cap S_{g_0}$, implies that $S_g = S_{g_0}$. □

Sketch of Theorem 3.2. Write $L_n(g)$ and $L(g)$ in (2.2) and (3.1) as

$$L_n(g) = \frac{N_n(g)}{D_n(g)}, \quad L(g) = \frac{N(g)}{D(g)} \tag{A.1}$$

where

$$N_n(g) = \frac{1}{n_1 n_2} \sum_{i=1}^{n_1} \sum_{j=1}^{n_2} \frac{1}{h_1} K_1 \left(\frac{t_i - g(s_j)}{h_1} \right) \frac{1}{h_2} K_2 \left(\frac{Y_{t_i} - Y'_{s_j}}{h_2} \right), \tag{A.2}$$

$$D_n(g) = \frac{1}{n_1 n_2} \sum_{i=1}^{n_1} \sum_{j=1}^{n_2} \frac{1}{h_1} K_1 \left(\frac{t_i - g(s_j)}{h_1} \right), \tag{A.3}$$

$$N(g) = \int_{-\infty}^{\infty} \int_{0}^{\infty} f_1(g(y)) f_2(y) f_{\epsilon_1}(v - m(g(y)) + m(g_0(y))) f_{\epsilon_2}(v) dy dv, \tag{A.4}$$

$$D(g) = \int_{0}^{\infty} f_1(g(y)) f_2(y) dy. \tag{A.5}$$

We have shown in the Supplementary Material that $N_n(g)$ tends to $N(g)$ and $D_n(g)$ tends to $D(g)$ in probability as $n \to \infty$ by showing that $E(N_n(g))$ and $E(D_n(g))$ tend to $N(g)$ and $D(g)$ respectively and $var(N_n(g))$ and $var(D_n(g))$ tend to zero as $n \to \infty$. The theorem then follows by the continuous mapping theorem of convergence in probability. □

***Lemma* A.1.** Let $f_{\epsilon_1+\epsilon_2}$ be the convolution of the densities f_{ϵ_1} and f_{ϵ_2}. Then under Assumption 3.1, $f_{\epsilon_1+\epsilon_2}$ is strictly unimodal at zero.

Proof. Fix $0 < u_1 < u_2$. By Assumption 3.1, we observe that

$$\begin{aligned}
& f_{\epsilon_1+\epsilon_2}(u_2) - f_{\epsilon_1+\epsilon_2}(u_1) \\
= & \int_{-\infty}^{\infty} f_{\epsilon_1}(v)\{f_{\epsilon_2}(u_2 - v) - f_{\epsilon_2}(v - u_1)\}dv \\
= & \int_{-\infty}^{\infty} f_{\epsilon_1}(u_1 + v)\{f_{\epsilon_2}(u_2 - u_1 - v) - f_{\epsilon_2}(v)\}dv \\
= & \int_{-\infty}^{\frac{u_2-u_1}{2}} f_{\epsilon_1}(u_1 + v)\{f_{\epsilon_2}(u_2 - u_1 - v) - f_{\epsilon_2}(v)\}dv \\
& \qquad + \int_{\frac{u_2-u_1}{2}}^{\infty} f_{\epsilon_1}(u_1 + v)\{f_{\epsilon_2}(u_2 - u_1 - v) - f_{\epsilon_2}(v)\}dv \\
= & \int_{\frac{u_2-u_1}{2}}^{\infty} f_{\epsilon_1}(u_2 - v)\{f_{\epsilon_2}(v) - f_{\epsilon_2}(u_2 - u_1 - v)\}dv \\
& \qquad + \int_{\frac{u_2-u_1}{2}}^{\infty} f_{\epsilon_1}(u_1 + v)\{f_{\epsilon_2}(u_2 - u_1 - v) - f_{\epsilon_2}(v)\}dv \\
= & \int_{\frac{u_2-u_1}{2}}^{\infty} \{f_{\epsilon_1}(u_2 - v) - f_1(u_1 + v)\}\{f_{\epsilon_2}(v) - f_{\epsilon_2}(u_2 - u_1 - v)\}dv \\
= & \int_0^{\infty} \left\{ f_{\epsilon_1}\left(\frac{u_2 + u_1}{2} - v\right) - f_{\epsilon_1}\left(\frac{u_2 + u_1}{2} + v\right)\right\} \\
& \qquad \times \left\{ f_{\epsilon_2}\left(\frac{u_2 - u_1}{2} + v\right) - f_{\epsilon_2}\left(\frac{u_2 - u_1}{2} - v\right)\right\} dv \\
< & \ 0.
\end{aligned}$$

By a similar argument, the same inequality holds for $u_2 < u_1 < 0$. □

Proof of Theorem 3.3. Observe from (3.1) and Assumption 3.1 that

$$L(g) = \frac{\int_0^{\infty} f_1(g(y))f_2(y)f_{\epsilon_1+\epsilon_2}(m(g(y)) - m(g_0(y)))dy}{\int_0^{\infty} f_1(g(y))f_2(y)dy}$$

where $f_{\epsilon_1+\epsilon_2}$ is as described in Lemma A.1. In particular, $L(g_0) = f_{\epsilon_1+\epsilon_2}(0)$. Thus,

$$\begin{aligned}
& L(g_0) - L(g) \\
= & \ \frac{\int_0^{\infty} f_1(g(x))f_2(x)\left[f_{\epsilon_1+\epsilon_2}(0) - f_{\epsilon_1+\epsilon_2}(m(g(x)) - m(g_0(x)))\right] dx}{\int_0^{\infty} f_1(g(x))f_2(x)dy}.
\end{aligned}$$

By Lemma A.1, $[f_{\epsilon_1+\epsilon_2}(0) - f_{\epsilon_1+\epsilon_2}(m(g(x)) - m(g_0(x)))] \geq 0$ for all x, which proves part (a).

In order that the last expression for $L(g_0) - L(g)$ happens to be zero for some $g \in \mathbb{G}_0$, the above difference must be equal to zero for all x such that $f_1(g(x))f_2(x) > 0$, i.e., for $x \in S_g \cap S_{g_0}$, where S_g is as defined at the beginning of Section 3. Since $f_{\epsilon_1+\epsilon_2}$ is strictly unimodal at 0, this requirement reduces to $m(g(x)) = m(g_0(x))$ for all $x \in S_g \cap S_{g_0}$. It follows from Theorem 3.1 that $S_g = S_{g_0}$ and $g(x) = g_0(x)$ for all $x \in S_{g_0}$, which establishes part (b). □

***Lemma* A.2.** Under Assumptions 3.1 and 3.5, the functional L in (3.1) is uniformly continuous on $\mathbb{G}$.

Proof. Let us recall the representation (A.1) of $L(g)$ and the expressions of $N(g)$ and $D(g)$ in (A.4) and (A.5) respectively. We first show that $N()$ is continuous on $\mathbb{G}$. Let $g \in \mathbb{G}$ and $\{g_k\}$ be a sequence of functions in $\mathbb{G}$ such that $\lim_{k\to\infty} \|g_k - g\| = 0$. By Assumption 3.1 it follows that the integrand in $N(g_k)$ is bounded by an integrable function $M_f^2 f_2(y) f_{\epsilon_2}(v)$. Further, by the continuity of f_1 and f_{ϵ_1} (Assumption 3.1), and m, and the fact that g_k converges to g pointwise, it follows that the integrand tends to $f_1(g(y))f_2(y)f_{\epsilon_1}(v - m(g(y)) + m(g_0(y)))f_{\epsilon_2}(v)$ as $k \to \infty$. Therefore, by dominating convergence theorem $\lim_{k\to\infty} N(g_k) = N(g)$ i.e. $N()$ is continuous on $\mathbb{G}$.

Similar arguments show that $D()$ is continuous as well. Further, by Assumption 3.1 and the expression of $D(g)$ in (A.5) we have that $D(g) > 0$ for all $g \in \mathbb{G}$. This gives that $L()$ is continuous on G. The lemma follows by Assumption 3.5. □ □

***Lemma* A.3.** Let the real numbers c and M_K' and the functionals L_n, N_n, D_n, N, and D are as defined earlier in this section. Then under Assumptions 3.1–3.6,

(a) for $g, \tilde{g} \in \mathbb{G}$,

$$|L_n(\tilde{g}) - L_n(g)| \leq B_n(\tilde{g})\|g - \tilde{g}\|$$

where

$$\begin{aligned} B_n(\tilde{g}) &= c^{-2} M_K^{'} \{N_n(\tilde{g}) + U_n D_n(\tilde{g})\} \\ U_n &= (n_1 n_2 h_2)^{-1} \sum_{i=1}^{n_1} \sum_{j=1}^{n_2} K_2\{(Y_{t_i} - Y'_{s_j})/h_2\}, \end{aligned}$$

(b) U_n tends to a constant U in probability as $n \to \infty$ where

$$U = \int_{-\infty}^{\infty} \int_0^{\infty} \int_0^{\infty} f_1(x) f_2(y) f_{\epsilon_1}(v - m(x) + m(g_0(y))) f_{\epsilon_2}(v) dx dy dv,$$

(c) $B_n(\tilde{g})$ tends to $B(\tilde{g})$ in probability as $n \to \infty$ where

$$B(\tilde{g}) = c^{-2} M_K^{'} \{N(\tilde{g}) + U D(\tilde{g})\}$$

.

Proof. Recall the positive real numbers c, M_K, M'_K as described at the beginning of Appendix.
From (A.3), we have $D_n(g) \geq c/h$. Using this inequality, from (A.1) we have,

$$|L_n(\tilde{g}) - L_n(g)| \leq \frac{h_1^2}{c^2} \left\{ D_n(\tilde{g}) \left| N_n(\tilde{g}) - N_n(g) \right| + N_n(\tilde{g}) \left| D_n(\tilde{g}) - D_n(g) \right| \right\}. \tag{A.6}$$

From (A.2) we have,

$$|N_n(\tilde{g}) - N_n(g)| \leq \frac{1}{n_1 n_2 h_1 h_2} \sum_{i=1}^{n1} \sum_{j=1}^{n2} K_2\left(\frac{Y_{t_i} - Y'_{s_j}}{h_2}\right) \left| K_1\left(\frac{t_i - \tilde{g}(s_j)}{h_1}\right) - K_1\left(\frac{t_i - g(s_j)}{h_1}\right) \right|,$$

which by mean value theorem and applying bounds of $K_1'()$ reduces to

$$|N_n(\tilde{g}) - N_n(g)| \leq \frac{M_K^{'}}{h_1^2} \|g - \tilde{g}\| U_n. \tag{A.7}$$

Similarly, from the expressions of $D_n(g)$ in (A.3) and by mean value theorem and applying bounds of $K_1'()$ we have

$$|D_n(\tilde{g}) - D_n(g)| \leq \frac{M_K^{'}}{h_1^2} \|g - \tilde{g}\|. \tag{A.8}$$

Part (a) follows by combining (A.7), (A.8) with (A.6).

From the expression of U_n in this Lemma, by (2.1) and Assumptions 3.1,

$$\begin{aligned} E(U_n) &= \int_{-\infty}^{\infty} \int_{-\infty}^{\infty} \int_0^{\infty} \int_0^{\infty} \frac{1}{h_2} K_2\left(\frac{m(x) - m(g_0(y)) + u - v}{h_2}\right) \\ &\times \quad f_1(x) f_2(y) f_{\epsilon_1}(u) f_{\epsilon_2}(v) dx dy du dv \\ &= \int_{-\infty}^{\infty} \int_{-\infty}^{\infty} \int_0^{\infty} \int_0^{\infty} K_2(w) f_1(x) f_2(y) \\ &\times \quad f_{\epsilon_1}(v - m(x) + m(g_0(y)) + w h_2) f_{\epsilon_2}(v) dx dy dw dv. \end{aligned}$$

By similar argument as in the proof of Theorem 3.2 at the beginning of this section, by Assumptions 3.1–3.4,

$$\lim_{n \to \infty} E(U_n) = U. \tag{A.9}$$

Write $var(U_n) = v_1(n) + v_2(n) + v_3(n) + v_4(n)$ where

$$v_1(n) = \frac{1}{(n_1 n_2 h_2)^2} \sum_{i=1}^{n_1} \sum_{j=1}^{n_2} var\left\{ K_2\left(\frac{Y_{t_i} - Y'_{s_j}}{h_2}\right) \right\},$$

$$v_2(n) = \frac{1}{(n_1 n_2 h_2)^2} \sum_{i=1}^{n_1} \sum_{j=1}^{n_2} \sum_{\substack{i'=1 \\ (\neq i)}}^{n_1} cov\left\{ K_2\left(\frac{Y_{t_i} - Y'_{s_j}}{h_2}\right), K_2\left(\frac{Y_{t_{i'}} - Y'_{s_j}}{h_2}\right) \right\},$$

$$v_3(n) = \frac{1}{(n_1n_2h_2)^2}\sum_{i=1}^{n_1}\sum_{j=1}^{n_2}\sum_{\substack{j'=1\\(\neq j)}}^{n_2} cov\left\{K_2\left(\frac{Y_{t_i}-Y'_{s_j}}{h_2}\right), K_2\left(\frac{Y_{t_i}-Y'_{s_{j'}}}{h_2}\right)\right\},$$

$$v_4(n) = \frac{1}{(n_1n_2h_2)^2}\sum_{i=1}^{n_1}\sum_{j=1}^{n_2}\sum_{\substack{i'=1\\(\neq i)}}^{n_1}\sum_{\substack{j'=1\\(\neq j)}}^{n_2} cov\left\{K_2\left(\frac{Y_{t_i}-Y'_{s_j}}{h_2}\right), K_2\left(\frac{Y_{t_{i'}}-Y'_{s_{j'}}}{h_2}\right)\right\}.$$

We show that all the above v_i's tend to zero as $n \to \infty$.

From the specifications of the model, it follows that $v_4(n) = 0$.

By a similar argument as in the proof of Theorem 3.2 at the beginning of this section, it follows that under Assumptions 3.1–3.4,

$$\begin{aligned}
\lim_{n\to\infty} n_1n_2h_2v_1(n) &= \int_{-\infty}^{\infty}K_2^2(w)dw\int_{-\infty}^{\infty}\int_0^{\infty}\int_0^{\infty}f_1(x)f_2(y)f_{\epsilon_1}(v-m(x)+m(g_0(y)))f_{\epsilon_2}(v)dxdydv,\\
\lim_{n\to\infty} n_2v_2(n) &= \int_{-\infty}^{\infty}\int_0^{\infty}f_2(y)f_{\epsilon_2}(v)\left\{\int_0^{\infty}f_1(x)f_{\epsilon_1}(v-m(x)+m(g_0(y)))dx\right\}^2dvdy-U^2,\\
\lim_{n\to\infty} n_1v_3(n) &= \int_{-\infty}^{\infty}\int_0^{\infty}f_1(x)f_{\epsilon_1}(v)\left\{\int_0^{\infty}f_2(y)f_{\epsilon_2}(v+m(x)-m(g_0(y)))dy\right\}^2dvdx-U^2
\end{aligned}$$

i.e.,

$$v_1(n) = O\left(\frac{1}{n_1n_2h_2}\right), \quad v_2(n) = O\left(\frac{1}{n_2}\right), \quad v_3(n) = O\left(\frac{1}{n_1}\right).$$

It completes the proof of part (b).

Part (c) follows from (**??**), (**??**), and (A.9). □

Proof of Theorem 3.4. By triangular inequality for any $g, \tilde{g} \in \mathbb{G}$ we have,

$$|L_n(g) - L(g)| \leq |L(\tilde{g}) - L(g)| + |L_n(g) - L_n(\tilde{g})| + |L_n(\tilde{g}) - L(\tilde{g})|. \tag{A.10}$$

Set $\epsilon > 0$. By Lemma A.2, there exists $\delta_\epsilon > 0$ such that $|L(g) - L(\tilde{g})| < \epsilon/3$ when $\|g - \tilde{g}\| < \delta_\epsilon$.

By Lemma A.3, $|L_n(\tilde{g}) - L_n(g)| \leq B_n(\tilde{g})\|g - \tilde{g}\|$ where as $n \to \infty$, $B_n(\tilde{g})$ goes to $B(\tilde{g})$ in probability which implies

$$\lim_{n\to\infty} pr\left\{B_n(\tilde{g}) > \max\left(\frac{\epsilon}{3\delta_\epsilon}, 2B(\tilde{g})\right)\right\} = 0. \tag{A.11}$$

For a given $\tilde{g} \in \mathbb{G}$, let $\delta(\tilde{g}, \epsilon) = \min\{(6B(\tilde{g}))^{-1}\epsilon, \delta_\epsilon\}$ if $B(\tilde{g}) > 0$ or δ_ϵ if $B(\tilde{g}) = 0$. Clearly $\{\mathcal{N}_{\delta(\tilde{g},\epsilon)}(\tilde{g}) : \tilde{g} \in \mathbb{G}\}$ is an open cover of $\mathbb{G}$ where $\mathcal{N}_\eta(\tilde{g}) = \{g : \|g - \tilde{g}\| < \eta\}$. By

Assumption 3.5, this cover contains a finite sub-cover say $\{\mathcal{N}_{\delta(\tilde{g}_j,\epsilon)}(\tilde{g}_j)\ j = 1 \dots k_\epsilon\}$ for some finite k_ϵ, of $\mathbb{G}$. Therefore, from (A.10)

$$\begin{aligned} & \sup_{g\in\mathbb{G}} |L_n(g) - L(g)| \\ \leq & \max_{j=1,\dots,k_\epsilon} \left\{ \sup_{g\in\mathcal{N}_{\delta(\tilde{g}_j,\epsilon)}(\tilde{g}_j)} |L(\tilde{g}_j) - L(g)| + \sup_{g\in\mathcal{N}_{\delta(\tilde{g}_j,\epsilon)}(\tilde{g}_j)} |L_n(g) - L_n(\tilde{g}_j)| + \sup_{g\in\mathcal{N}_{\delta(\tilde{g}_j,\epsilon)}(\tilde{g}_j)} |L_n(\tilde{g}_j) - L(\tilde{g}_j)| \right\} \\ \leq & \frac{\epsilon}{3} + \max_{j=1,\dots,k_\epsilon} \delta(\tilde{g}_j,\epsilon) B_n(\tilde{g}_j) + \sum_{j=1}^{k_\epsilon} |L_n(\tilde{g}_j) - L(\tilde{g}_j)|. \end{aligned}$$

Consequently,

$$\begin{aligned} & pr\left(\sup_{g\in\mathbb{G}} |L_n(g) - L(g)| > \epsilon \right) \\ \leq & \sum_{j=1}^{k_\epsilon} pr\left(B_n(\tilde{g}_j) > \frac{\epsilon}{3\delta(\tilde{g}_j,\epsilon)} \right) + pr\left(\sum_{j=1}^{k_\epsilon} |L_n(\tilde{g}_j) - L(\tilde{g}_j)| > \frac{\epsilon}{3} \right). \end{aligned}$$

Each summand of the first term goes to zero by (A.11), while those of the second term goes to zero by Theorem 3.2. □

Proof of Theorem 3.5. Fix $\epsilon > 0$. We have

$$\begin{aligned} & pr(|L_n(\hat{g}_n) - L(g_0)| > \epsilon) \\ \leq & pr(|L_n(\hat{g}_n) - L(g_0)| > \epsilon, |L_n(g_0) - L(g_0)| \leq \epsilon, |L_n(\hat{g}_n) - L(\hat{g}_n)| \leq \epsilon) \\ & + pr(|L_n(\hat{g}_n) - L(\hat{g}_n)| > \epsilon) + pr(|L_n(g_0) - L(g_0)| > \epsilon), \end{aligned} \tag{A.12}$$

where $\hat{g}_n$ is as in (2.3). We show that all the three terms on the right side of (A.12) are arbitrarily small.

From (2.3), we have $L_n(g_0) \leq L_n(\hat{g}_n)$. Thus, if $|L_n(g_0) - L(g_0)| \leq \epsilon$, $L_n(\hat{g}_n) \geq L(g_0) - \epsilon$. By Theorem 3.3(a), if $|L_n(\hat{g}_n) - L(\hat{g}_n)| \leq \epsilon$ then $L_n(\hat{g}_n) \leq L(g_0) + \epsilon$. Therefore, if $|L_n(g_0) - L(g_0)| \leq \epsilon$ and $|L_n(\hat{g}_n) - L(\hat{g}_n)| \leq \epsilon$ then $|L_n(\hat{g}_n) - L(g_0)| \leq \epsilon$, which makes the first term on the right side of (A.12) zero. Observing that $|L_n(\hat{g}_n) - L(\hat{g}_n)| \leq \sup_{g\in\mathbb{G}} |L_n(g) - L(g)|$, by Theorem 3.4 the second term tends to zero while by Theorem 3.2 the last term goes to zero as $n \to \infty$. □

Proof of Theorem 3.6. Suppose that $\hat{g}_n$ does not tend to g_0 in probability as $n \to \infty$, i.e. there exists an $\epsilon > 0$ and a $\delta > 0$ such that $P\{\|\hat{g}_n - g_0\| \geq \epsilon\} > \delta$ infinitely often. Consider a closed subset $\mathcal{N}_\epsilon^c(g_0) = \{g : \|g - g_0\| \geq \epsilon,\ g \in \mathbb{G}\}$. By Assumption 3.5 and Lemma A.2, there exists a $\tilde{g} \in \mathcal{N}_\epsilon^c(g_0)$ such that $\tilde{g} = \operatorname{argmax}_{g\in\mathcal{N}_\epsilon^c(g_0)} L(g)$. Denote $\eta = L(g_0) - L(\tilde{g})$. By Theorem 3.3(b), $\eta > 0$. We have $|L_n(\hat{g}_n) - L(g_0)| \geq |L(g_0) - L(\hat{g}_n)| - |L_n(\hat{g}_n) - L(\hat{g}_n)|$. Thus,

if $\hat{g}_n \in \mathcal{N}_\epsilon^c(g_0)$ and $\sup_{g\in\mathbb{G}} |L_n(g) - L(g)| < \eta/2$ then $|L_n(\hat{g}_n) - L(g_0)| > \eta/2$. Consequently,

$$\begin{aligned} & pr\left\{|L_n(\hat{g}_n) - L(g_0)| > \frac{\eta}{2}\right\} \\ \geq \quad & pr\{\|\hat{g}_n - g_0\| \geq \epsilon\} + pr\left\{\sup_{g\in\mathbb{G}} |L_n(g) - L(g)| < \frac{\eta}{2}\right\} - 1. \end{aligned}$$

The first term on the right hand side is greater than δ infinitely often while by Theorem 3.4, the second term is greater than $1 - \frac{\delta}{2}$ for all but finitely many n. Therefore, $pr(|L_n(\hat{g}_n) - L(g_0)| > \eta/2) > \delta/2$ infinitely often, which contradicts Theorem 3.5. □

Acknowledgement

The work of Srivastava was supported in part by INSPIRE research grant from DST of Government of India and a research seed grant from the Indian Institute of Technology, Bombay.

References

[1] Bigot, J. (2006) Landmark-based registration of curves via the continuous wavelet transform.*J. Comput. Graph. Statist.*, **15**, 542–564.

[2] Brumback, L. C. and Lindstrom, M. J. (2004) Self modeling with flexible, random time transformations.*Biometrics*, **60**, 461–470.

[3] Eubank, R. L. (1999) Nonparametric Regression and Spline Smoothing (2 ed.). New York: Marcel Dekker, Inc.

[4] Gervini, D. and Gasser, T. (2004) Self-modelling warping functions.*J. R. Statist. Soc.* B **66**, 959–971.

[5] Gervini, D. and Gasser, T. (2005) Nonparametric maximum likelihood estimation of the structural mean of a sample of curves.*Biometrika*, **92**, 801–820.

[6] James, G. M.(2007) Curve alignment by moments.*Ann. Appl. Statist.* **1**, 480–501.

[7] Kneip, A. and Engel, J.(1995) Model estimation in nonlinear regression under shape invariance.*Ann. Statist.* **23**, 551–570.

[8] Kneip, A. and Gasser, T.(1992) Statistical tools to analyze data representing a sample of curves.*Ann. Statist.* **20**, 1266–1305.

[9] Kneip, A.and Ramsay, J. O. (2008) Combining registration and fitting for functional models.*J. Am. Statist. Assoc.* **103**, 1155–1165.

[10] Kneip, A., Li, X., MacGibbon, K. B. and Ramsay, J. O.(2000) Curve registration by local regression.*Can. J. Statist.* **28**, 19–29.

[11] Liu, X. and Müller, H.-G.(2004) Functional convex averaging and synchronization for time-warped random curves.*J. Am. Statist. Assoc.* **99**, 687–699.

[12] Loulergue, L., Schilt, A., Spahni, R., Masson-Delmotte, V., Blunier, T.,Lemieux, B., Barnola, J.-M., Raynaud, D., Stocker, T. and Chappellaz, J. (2008) Orbital and millennial-scale features of atmospheric ch4 over the past 800,000 years.*Nature*, **453**, 383–386.

[13] Lüthi, D., Floch, M. L., Bereiter, B., Blunier, T., Barnola, J. M., Siegenthaler, U., Raynaud, D., Jouzel, J., Fischer, H., Kawamura, K. and Stocker, T. (2008) High-resolution carbon dioxide concentration record 650,000-800,000 years before present.*Nature*, **453**, 379–382.

[14] Masson-Delmotte, V. (2007) Lsce/ipsl igbp pages/wdca contribution. 2007-091.

[15] Petit, J. R., Jouzel, J., Raynaud, D., Barkov, N. I., Barnola, J. M., Basile, I., Bender, M., Chappellaz, J., Davis, M., Delaygue, G., Delmotte, M., Kotlyakov, V. M., Legrand, M., Lipenkov, V. Y., Lorius, C., Pepin, L., Ritz, C., Saltzman, E. and Stievenard, M. (1999) Climate and atmospheric history of the past 420,000 years from the vostok ice core, Antarctica.*Nature*, **399**, 429–436.

[16] Ramsay, J. O. and Li, X. (1998) Curve registration.*J. R. Statist. Soc.* B **60**,351–363.

[17] Rønn, B. B. (2001) Nonparametric maximum likelihood estimation for shifted curves.*J. R. Statist. Soc.* B **63**,243–259.

[18] Silverman, B. W.(1995) Incorporating parametric effects into functional principal components analysis.*J. R. Statist. Soc.* B **57**,673–689.

[19] Tang, R. and Müller, H. G.(2008) Pairwise curve synchronization for functional data.*Biometrika*, **95**, 875–889.

[20] Wang, K. and Gasser, T. (1997) Alignment of curves by dynamic time warping.*Ann. Statist.*, **25**, 1251–1276.

[21] Wang, K. and Gasser, T. (1999) Synchronizing sample curves nonparametrically.*Ann. Statist.* **27**, 439–460.

arXiv:1704.03127v1 [stat.ME] 11 Apr 2017

Supplementary material for Feature Sensitive Curve Registration by Maximizing Kernel based Matching Scores

***Proof of Theorem* ??.** From (**??**), by (**??**) and Assumption **??**,

$$\begin{aligned} E(N_n(g)) &= \int_{-\infty}^{\infty}\int_{-\infty}^{\infty}\int_{0}^{\infty}\int_{0}^{\infty} \frac{1}{h_1}K_1\left(\frac{x-g(y)}{h_1}\right)\frac{1}{h_2}K_2\left(\frac{m(x)-m(g_0(y))+u-v}{h_2}\right) \\ &\times \; f_1(x)f_2(y)f_{\epsilon_1}(u)f_{\epsilon_2}(v)dxdydudv \\ &= \int_{-\infty}^{\infty}\int_{0}^{\infty}\int_{-\infty}^{\infty}\int_{-\infty}^{\infty} I_{\left(\frac{-g(y)}{h_1},\infty\right)}(z_1)K_1(z_1)\,K_2(z_2)\,f_1(g(y)+z_1h_1) \\ &\times \; f_2(y)f_{\epsilon_1}(v-m(g(y)+z_1h_1)+m(g_0(y))+z_2h_2)f_{\epsilon_2}(v)dz_1dz_2dydv. \end{aligned}$$

This integrand is bounded by an integrable function namely

$$M_f^2K_1(z_1)K_2(z_2)f_2(y)f_{\epsilon_2}(v)$$

, where the real number M_f is as described at the beginning of Appendix. Observe that, as g is a positive function, any given z_1 is contained in $(-g(y)/h_1,\infty)$ for sufficiently small h_1. Hence by Assumptions **??**, **??**, **??**, and continuity of m, for a fixed (z_1,z_2,y,v), the integrand tends to $K_1(z_1)K_2(z_2)f_1(g(y))f_2(y)f_{\epsilon_1}(v-m(g(y))+m(g_0(y)))f_{\epsilon_2}(v)$ as $n\to\infty$. Consequently, by dominating convergence theorem and Assumptions **??**–**??**,

$$\lim_{n\to\infty} E(N_n(g)) = N(g) \tag{1}$$

where $N(g)$ is as in (**??**).

From (**??**), by (**??**) and Assumption **??**,

$$E(D_n(g)) = \int_{0}^{\infty}\int_{-\infty}^{\infty} I_{\left(\frac{-g(y)}{h_1},\infty\right)}(z)K_1(z)f_1(g(y)+zh_1)f_2(y)dzdy.$$

By a similar argument as above, by Assumptions **??**–**??**,

$$\lim_{n\to\infty} E(D_n(g)) = D(g) \tag{2}$$

where $D(g)$ is as in (**??**).

Write $var(N_n(g)) = v_1(n) + v_2(n) + v_3(n) + v_4(n)$ where

$$v_1(n) = \frac{1}{(n_1 n_2 h_1 h_2)^2} \sum_{i=1}^{n1} \sum_{j=1}^{n2} var \left\{ K_1 \left(\frac{t_i - g(s_j)}{h_1} \right) K_2 \left(\frac{Y_{t_i} - Y'_{s_j}}{h_2} \right) \right\}, \quad (3)$$

$$v_2(n) = \frac{1}{(n_1 n_2 h_1 h_2)^2} \sum_{i=1}^{n1} \sum_{j=1}^{n2} \sum_{\substack{i'=1 \\ (\neq i)}}^{n1} cov \left\{ K_1 \left(\frac{t_i - g(s_j)}{h_1} \right) K_2 \left(\frac{Y_{t_i} - Y'_{s_j}}{h_2} \right), \right.$$
$$\left. K_1 \left(\frac{t_{i'} - g(s_j)}{h_1} \right) K_2 \left(\frac{Y_{t_{i'}} - Y'_{s_j}}{h_2} \right) \right\}, \quad (4)$$

$$v_3(n) = \frac{1}{(n_1 n_2 h_1 h_2)^2} \sum_{i=1}^{n1} \sum_{j=1}^{n2} \sum_{\substack{j'=1 \\ (\neq j)}}^{n2} cov \left\{ K_1 \left(\frac{t_i - g(s_j)}{h_1} \right) K_2 \left(\frac{Y_{t_i} - Y'_{s_j}}{h_2} \right), \right.$$
$$\left. K_1 \left(\frac{t_i - g(s_{j'})}{h_1} \right) K_2 \left(\frac{Y_{t_i} - Y'_{s_{j'}}}{h_2} \right) \right\}, \quad (5)$$

$$v_4(n) = \frac{1}{(n_1 n_2 h_1 h_2)^2} \sum_{i=1}^{n1} \sum_{j=1}^{n2} \sum_{\substack{i'=1 \\ (\neq i)}}^{n1} \sum_{\substack{j'=1 \\ (\neq j)}}^{n2} cov \left\{ K_1 \left(\frac{t_i - g(s_j)}{h_1} \right) K_2 \left(\frac{Y_{t_i} - Y'_{s_j}}{h_2} \right) \right.$$
$$\left. K_1 \left(\frac{t_{i'} - g(s_{j'})}{h_1} \right) K_2 \left(\frac{Y_{t_{i'}} - Y'_{s_{j'}}}{h_2} \right) \right\}.$$

We show that each of the $v_i(n)$'s tends to zero as $n \to \infty$.

From the model specifications it follows that $v_4(n) = 0$.

From (3), by (**??**) and Assumption **??**,

$$v_1(n) = \frac{1}{n_1 n_2 h_1 h_2} v_{11}(n) - \frac{1}{n_1 n_2} E^2(N_n(g))$$

where

$$v_{11}(n) = \int_{-\infty}^{\infty} \int_{0}^{\infty} \int_{-\infty}^{\infty} \int_{-\infty}^{\infty} I_{\left(\frac{-g(y)}{h_1}, \infty\right)}(z_1) K_1^2(z_1) K_2^2(z_2) f_1(g(y) + z_1 h_1)$$
$$\times \; f_2(y) f_{\epsilon_1}(v - m(g(y) + z_1 h_1) + m(g_0(y)) + z_2 h_2) f_{\epsilon_2}(v) dz_1 dz_2 dy dv.$$

By a similar argument as at the beginning of this proof, by Assumptions **??–??**,

$$\lim_{n \to \infty} n_1 n_2 h_1 h_2 v_1(n) = \int_{-\infty}^{\infty} K_1^2(z_1) dz_1 \int_{-\infty}^{\infty} K_2^2(z_2) dz_2$$
$$\times \int_{-\infty}^{\infty} \int_{0}^{\infty} f_1(g(y)) f_2(y) f_{\epsilon_1}(v - m(g(y)) + m(g_0(y))) f_{\epsilon_2}(v) dy dv$$

i.e.,

$$v_1(n) = O\left(\frac{1}{n_1 n_2 h_1 h_2}\right).$$

Arguing in a similar manner as above, from (4)–(5), by (**??**) and Assumptions **??**–**??**,

$$\begin{aligned}
\lim_{n\to\infty} n_2 v_2(n) &= \int_0^\infty \int_{-\infty}^\infty f_1^2(g(y)) f_2(y) f_{\epsilon_1}^2(v - m(g(y)) + m(g_0(y))) f_{\epsilon_2}(v) dv dy - N^2(g), \\
\lim_{n\to\infty} n_1 v_3(n) &= \int_0^\infty \int_{-\infty}^\infty \frac{f_2^2(y)}{g'(y)} f_1(g(y)) f_{\epsilon_1}(v - m(g(y)) + m(g_0(y))) f_{\epsilon_2}^2(v) dv dy - N^2(g)
\end{aligned}$$

i.e.,

$$v_2(n) = O\left(\frac{1}{n_2}\right), \quad v_3(n) = O\left(\frac{1}{n_1}\right).$$

Write $var(D_n(g)) = v_1^*(n) + v_2^*(n) + v_3^*(n) + v_4^*(n)$ where

$$v_1^*(n) = \frac{1}{(n_1 n_2 h_1)^2} \sum_{i=1}^{n1} \sum_{j=1}^{n2} var\left\{K_1\left(\frac{t_i - g(s_j)}{h_1}\right)\right\}, \tag{6}$$

$$v_2^*(n) = \frac{1}{(n_1 n_2 h_1)^2} \sum_{i=1}^{n1} \sum_{j=1}^{n2} \sum_{\substack{i'=1 \\ (\neq i)}}^{n1} cov\left\{K_1\left(\frac{t_i - g(s_j)}{h_1}\right), K_1\left(\frac{t_{i'} - g(s_j)}{h_1}\right)\right\}, \tag{7}$$

$$v_3^*(n) = \frac{1}{(n_1 n_2 h_1)^2} \sum_{i=1}^{n1} \sum_{j=1}^{n2} \sum_{\substack{j'=1 \\ (\neq j)}}^{n2} cov\left\{K_1\left(\frac{t_i - g(s_j)}{h_1}\right), K_1\left(\frac{t_i - g(s_{j'})}{h_1}\right)\right\}, \tag{8}$$

$$v_4^*(n) = \frac{1}{(n_1 n_2 h_1)^2} \sum_{i=1}^{n1} \sum_{j=1}^{n2} \sum_{\substack{i'=1 \\ (\neq i)}}^{n1} \sum_{\substack{j'=1 \\ (\neq j)}}^{n2} cov\left\{K_1\left(\frac{t_i - g(s_j)}{h_1}\right), K_1\left(\frac{t_{i'} - g(s_{j'})}{h_1}\right)\right\}.$$

We show that all the $v_i^*(n)$'s tend to zero as $n \to \infty$.

From the model specifications, $v_4^*(n) = 0$.

From (6), by (**??**) and Assumption **??**,

$$v_1^*(n) = \frac{1}{n_1 n_2 h_1} v_{11}^*(n) - \frac{1}{n_1 n_2} E^2(D_n(g))$$

where

$$v_{11}^*(n) = \int_0^\infty \int_{-\infty}^\infty I_{\left(\frac{-g(y)}{h_1}, \infty\right)}(z) K_1^2(z) f_1(g(y) + h_1 z) f_2(y) dz dy.$$

Arguing in a similar manner as in the case of $var(v_1(n))$ above, by Assumptions **??**–**??**,

$$\lim_{n\to\infty} n_1 n_2 h_1 v_1^*(n) = \int_{-\infty}^\infty K_1^2(z) dz \int_0^\infty f_1(g(y)) f_2(y) dy$$

i.e.,

$$v_1^*(n) = O\left(\frac{1}{n_1 n_2 h_1}\right).$$

By a similar argument as above, from (7)–(8), by (**??**) and Assumptions **??**–**??**,

$$\lim_{n\to\infty} n_2 v_2^*(n) = \int_0^\infty f_1^2(g(y)) f_2(y) dy - D^2(g),$$
$$\lim_{n\to\infty} n_1 v_3^*(n) = \int_0^\infty \frac{f_1(g(y)) f_2^2(y)}{g'(y)} dy - D^2(g)$$

i.e.,

$$v_2^*(n) = O\left(\frac{1}{n_2}\right), \quad v_3^*(n) = O\left(\frac{1}{n_1}\right).$$

It completes the proof. □